Reactivity of the P–N Bond in the Halide Salts of Bis[bis(diphenylphosphino)methylamine]platinum(II)†

C. Scott Browning and David H. Farrar*
Department of Chemistry, University of Toronto, Toronto, Ontario M5S 1A1, Canada

Conductivity measurements and $^{31}P-\{^{1}H\}$ NMR spectroscopy suggested that the chloride and iodide salts of bis[bis(diphenylphosphino)methylamine]platinum(II) $[Pt(dppma)_2]^{2+}$ **1** exist in solution equilibrium with the five-co-ordinate complexes $[Pt(dppma)_2X]^+$ (X = Cl or I). The magnitude of the interaction of the iodide ion with **1** is greater than that of the chloride ion. The extent of formation of the halide-associated species is dependent upon the nature of the solvent. Association equilibrium constants K_{assoc} = 0.0718 and 0.315 mol dm^{-3} respectively were calculated for the chloride and iodide salts of **1** in $MeNO_2$. Addition of trace quantities of water to solutions of the chloride or iodide salts of **1** effected cleavage of both P–N bonds of one of its dppma ligands giving $[Pt(dppma)\{(Ph_2PO)_2H\}]^+$ **2**. The structure of the cation was investigated crystallographically as a mixture of the iodide and tetrafluoroborate salts of the form $I_{0.21}[BF_4]_{0.79}$. The analogous reaction of the chloride salt of **1** with MeOH produces cleavage of only one P–N bond to give $[Pt(dppma)(Ph_2POMe)(Ph_2PNHMe)]^{2+}$ **3** as the chloride salt. Phosphorus–nitrogen bond solvolysis of both ligands of **1** occurs to give the complex *trans*-$[Pt(Ph_2POMe)_2(CN)_2]$ **4** upon addition of 2 equivalents of sodium cyanide to methanolic solvent mixtures of $[Pt(dppma)_2]X_2$ (X = BF_4, Cl or I). The product was characterised crystallographically. Possible mechanisms of formation of these complexes are discussed.

The hydrolytic instability of the P–N bond of phosphazanes is well known.[1] Both experimental[1,2] and theoretical[3] studies remain inconclusive as to the mechanism by which this process occurs. In his studies of the transition-metal co-ordination chemistry of chelating derivatives of PF_3, King[4] observed solvolysis of co-ordinated phosphazanes in the P–N bond-cleavage reactions of the bidentate ligand $F_2PN(Me)PF_2$ by protic solvents. The reactions of $[Mo(\eta^5\text{-}C_5H_5)(CO)_3Cl]$ and $[Fe(\eta^5\text{-}C_5H_5)(CO)_2Cl]$ with $NMe(PF_2)_2$ in the presence of small amounts of alcohol ROH (R = Me or Et) yielded the complexes $[Mo(\eta^5\text{-}C_5H_5)(CO)_2(F_2PNHMe)Cl]$ and $[Fe(\eta^5\text{-}C_5H_5)(CO)(F_2PNHMe)Cl]$, respectively.[5] The products of the same reactions carried out in the absence of alcohol possessed monodentate co-ordination of the diphosphinoamine ligand.[5]

During our investigations of the Group 10 co-ordination chemistry of derivatives of the compound bis(diphenylphosphino)amine we have observed a susceptibility of the P–N bond of the complex bis[bis(diphenylphosphino)methylamine]platinum(II), $[Pt(dppma)_2]^{2+}$ **1**, toward solvolysis in protic media. The conditions associated with this reactivity of the P–N bonds of **1** are reported herein. Interestingly, bis[bis(diphenylphosphino)amine]platinum(II), $[Pt(dppa)_2]^{2+}$, does not exhibit this behaviour under identical reaction conditions. Crystallographically characterised examples of P–N bond cleavage of one and both of the dppma ligands of **1** are described in the solid-state structures of the complexes $[Pt(dppma)\{(Ph_2PO)_2H\}]I_{0.21}[BF_4]_{0.79}$ and $[Pt(Ph_2PO\text{-}Me)_2(CN)_2]$. The synthesis and characterisation of halide and tetrafluoroborate salts of **1** have been previously described.[6]

Results and Discussion

Evidence for the Formation of the Five-co-ordinate Species $[Pt(dppma)_2X]^+$ (X = Cl *or* I).—As solutions of the tetrafluoroborate salt of complex **1** are colourless, evidence of its intimate association with halide ions is immediately apparent in the bright yellow and intense yellow-orange CH_2Cl_2 solutions of the chloro and iodo salts, respectively. In the solid state the chloride salt is colourless while the iodide salt is pale yellow. The stability of halide-associated species is also evident in the gas phase. The *m/z* values of the molecular ion peak in the FAB mass spectra of the halide salts are consistent with the species $[Pt(dppma)_2X]^+$ (X = Cl or I) whereas the molecular ion of the BF_4^- salt shows no such association (Table 1).

The conductivities and ^{31}P NMR spectroscopic properties of the chloride, iodide and tetrafluoroborate salts of **1** were measured to determine the degree of halide association in solutions of these complexes. The molar conductivity data, Λ_m, were collected by measurement of the specific conductance of

Table 1 Solution ^{31}P NMR spectroscopic[a] and FAB mass spectrometric[b] molecular-ion data for $[Pt(dppma)_2]X_2$ (X = Cl, I or BF_4) and complexes **2–4**

Complex	δ[c]	$\lvert^1J(P\text{–}Pt)\rvert$/Hz	Molecular ion (*m/z*)
1 (BF_4^- salt)	39.3	2139	$[\mathbf{1}]^+$ (994)
(Cl^- salt)	31.2	2297	$[\mathbf{1} + Cl^-]^+$ (1029)
(I^- salt)	21.4	2367	$[\mathbf{1} + I^-]^+$ (1121)
2	—[d]	—[d]	$[\mathbf{2} - H]^+$ (997)
3	—[e]	—[e]	$[\mathbf{3} + H]^+$ (1026)
4	100.8	2548	$[\mathbf{4}]^+$ (680)

[a] CH_2Cl_2 at 20 °C. [b] Xenon gas ionising source at 8 kV and 1 mA; 3-nitrobenzyl alcohol matrix. [c] Values relative to 85% H_3PO_4. [d] See Scheme 1 for phosphorus atom assignments: $\delta(P_A)$ 41.4, $\delta(P_B)$ 64.7; $|^1J(P_A\text{–}Pt)| = |^1J(P_{A'}\text{–}Pt)| = 1849$, $|^1J(P_B\text{–}Pt)| = |^1J(P_{B'}\text{–}Pt)| = 2722$, $|^2J(P_A\text{–}P_B)| = |^2J(P_{A'}\text{–}P_{B'})| = 350$, $|^2J(P_A\text{–}P_{A'})| = 39$, $|^2J(P_A\text{–}P_{B'})| = |^2J(P_{A'}\text{–}P_B)| = 14$, $|^2J(P_B\text{–}P_{B'})| = 28$ Hz. [e] See Scheme 1 for phosphorus atom assignments: $\delta(P_A)$ 37.4, $\delta(P_B)$ 43.1, $\delta(P_C)$ 106.8, $\delta(P_D)$ 49.9; $|^1J(P_A\text{–}Pt)| = 2396$, $|^1J(P_B\text{–}Pt)| = 1404$, $|^1J(P_C\text{–}Pt)| = 3422$, $|^1J(P_D\text{–}Pt)| = 2596$, $|^2J(P_A\text{–}P_B)| = 37$, $|^2J(P_A\text{–}P_C)| = 420$, $|^2J(P_A\text{–}P_D)| = 10$, $|^2J(P_B\text{–}P_C)| = 28$, $|^2J(P_B\text{–}P_D)| = 353$, $|^2J(P_C\text{–}P_D)| = 23$ Hz.

† *Supplementary data available:* see Instructions for Authors, *J. Chem. Soc., Dalton Trans.*, 1995, Issue 1, pp. xxv–xxx.

Table 2 Conductivity values Λ_m obtained at concentration, c, for nitromethane solutions of $[Pt(dppma)_2]X_2$ (X = Cl, I or BF_4)

X	c/mmol dm^{-3}	Λ_m/S cm^2 mol^{-1}
Cl	0.390	169
	0.974	161
	1.95	151
	4.87	138
	9.74	127
I	0.398	171
	0.995	155
	1.99	141
	4.97	121
	9.95	107
BF_4	0.400	170
	1.00	162
	2.00	154
	5.00	141
	10.0	122

the solutions over a range of concentrations,[7] c. The application of the Onsager conductivity relation (1) gave the limiting molar

$$\Lambda_m = (\Lambda_m)_0 - ac^{\frac{1}{2}} \quad (1)$$

conductivity at infinite dilution, $(\Lambda_m)_0$. The conductivity data are presented in Table 2: $(\Lambda_m)_0$ and Λ_m (10^{-3} mol dm^{-3}) were respectively extrapolated and interpolated from a least-squares linear regression fit of the data. The values, which are given in Table 3, clearly fall within the accepted[7] range of $(\Lambda_m)_0$ = 115–250 S cm^2 mol^{-1} and Λ_m (10^{-3} mol dm^{-3}) = 150–180 S cm^2 mol^{-1} for 2:1 electrolytes. These values contrast those obtained[8] from conductivity measurements of $MeNO_2$ solutions of the analogous salts of $[Pt(dppm)_2]^{2+}$ (dppm = $Ph_2PCH_2PPh_2$) (Table 3) which suggest that the five-co-ordinate cation $[Pt(dppm)_2X]^+$ (X = Cl, Br or I) represents the dominant species in solution.

The combined conductive and chromatic properties of the complexes suggest that, in solution, coloured $[Pt(dppma)_2X]^+$ exists in an equilibrium (2) with its conjugate Lewis acid dication which favours the latter species.

$$[Pt(dppma)_2X]^+ \rightleftharpoons [Pt(dppma)_2]^{2+} + X^- \quad (2)$$

The chemical equivalence of the phosphorus nuclei observed as a singlet with ^{195}Pt-coupled satellite resonances in the ^{31}P NMR spectrum of the BF_4^- salt of complex **1** (Table 1) is maintained in its halide salts. The chemical shift and $|^1J(P–Pt)|$ coupling of the chloride and iodide salts of **1** exhibit a dependence upon the nature of the solvent as shown in Table 4 which is consistent with the existence of the equilibrium (2). Although no inference regarding the degree of association in the BF_4^- salt of **1** may be made from the conductivity data[9] exclusively, the invariance of its NMR parameters with changes in the nature of the solvent suggests that little counter-ion association or ion pairing occurs in its solutions. The consistency of the NMR data of the BF_4^- salt of **1** also offers no evidence of covalent interactions between the solvent and the free complex. The participation of the solvent in such a capacity has been observed in the formation of $[Pt(dppm)_2(CD_3CN)]^{2+}$ in deuteriated acetonitrile.[8] Hydrogen bonding may be of significance in solvating free halide ions[10] as the NMR parameter values of the halide salts of **1** in methanol approach (X = Cl) or closely approach (X = I) those of the BF_4^- salt.

The single sharp resonance, with ^{195}Pt-coupled satellites, in the ^{31}P NMR solution spectra of the halide salts indicates that equilibrium (2) proceeds at the fast-exchange limit on the NMR frequency scale at room temperature. The absence of a significant change in lineshape upon cooling of a solution of the iodide salt of complex **1** to temperatures as low as −80 °C reflects the lability of the halide association/dissociation process.

Table 3 Molar conductivity data for $[Pt(dppma)_2]X_2$ (X = Cl, I or BF_4) and $[Pt(dppm)_2]X_2$ (X = Cl or I)[a] in $MeNO_2$

	$[Pt(dppma)_2]^{2+}$		$[Pt(dppm)_2]^{2+}$	
X	$(\Lambda_m)_0$[b]	Λ_m[b] (10^{-3} mol dm^{-3})	$(\Lambda_m)_0$[b]	(Λ_m)[b] (10^{-3} mol dm^{-3})
Cl	177	160	86	78
I	181	156	82	79
BF_4	181	163	—	—

[a] Ref. 8. [b] Units S cm^2 mol^{-1}.

Table 4 Solvent dependence of the ^{31}P NMR chemical shift and $|^1J(Pt–P)|$ coupling constant of the complexes $[Pt(dppma)_2]X_2$ (X = Cl, I or BF_4) upon the nature of the counter ion and solvent ($c \approx 0.001$ mol dm^{-3})

X	Solvent	δ[a]	$\Delta\delta$[b]	$\lvert^1J(Pt–P)\rvert$/Hz	$\Delta\lvert^1J(Pt–P)\rvert$[c]/Hz
Cl	CH_2Cl_2	31.2	—	2297	—
	Me_2SO	36.5	5.3	2188	−109
	$MeNO_2$	39.8	8.6	2156	−141
	MeOH	41.6	10.4	2128	−169
I	CH_2Cl_2	21.4	—	2367	—
	Me_2SO	33.3	11.9	2218	−149
	$MeNO_2$	34.5	13.1	2216	−151
	MeOH	37.2	15.8	2162	−205
BF_4	CH_2Cl_2	39.3	—	2139	—
	Me_2SO	38.6	−0.7	2129	−10
	$MeNO_2$	40.6	1.3	2137	−2
	MeOH[d]	—	—	—	—

[a] Values relative to 85% H_3PO_4. [b] $\Delta\delta = |\delta_{solvent} - \delta_{CH_2Cl_2}|$. [c] $\Delta|^1J(Pt–P)| = |^1J(Pt–P)_{solvent}| - |^1J(Pt–P)_{CH_2Cl_2}|$. [d] Insoluble.

The ^{31}P NMR spectra of the chloride and iodide salts of complex **1** were acquired as CH_2Cl_2 solutions in the presence of a > 100-fold excess of the appropriate halide, as NBu^n_4X, to displace the equilibrium toward the formation of $[Pt(dppma)_2X]^+$. Chemical shifts of δ 33.3 and 24.2 and Pt–P coupling constants of $|^1J(P–Pt)| = 2264$ and 2340 Hz were thereby obtained for $[Pt(dppma)_2Cl]^+$ and $[Pt(dppma)_2I]^+$, respectively. The similarities of the chemical shifts and $|^1J(P–Pt)|$ coupling constants with the values measured in the absence of supplementary halide (Table 4) suggests that formation of the five-co-ordinate species is effectively complete in the neat CH_2Cl_2 solutions of the halide salts.

The degree of halide association in the $MeNO_2$ solutions of both salts and the corresponding equilibrium constant, K_{assoc}, for equation (2) may then be calculated from the $|^1J(P–Pt)|$ values of the ^{31}P NMR spectrum using equation (3) in which

$$J_{obs} = xJ_{Pt^{2+}} + (1 - x)J_{PtX^+} \quad (3)$$

$J_{Pt^{2+}}$ and J_{PtX^+} are the $^1J(P–Pt)$ coupling constants* of the pure complexes $[Pt(dppma)_2]^{2+}$ and $[Pt(dppma)_2X]^+$, respectively, x is the fraction of species in solution present as $[Pt(dppma)_2]^{2+}$ at equilibrium and J_{obs} is the observed $^1J(P–Pt)$ coupling constant of the dissolved salt. The value of $J_{Pt^{2+}}$ is taken to be that of the BF_4^- salt ($J_{Pt^{2+}} = 2139$ Hz). The J_{PtX^+} values of 2367 (X = I) and 2297 Hz (X = Cl) yield $[Pt(dppma)_2X]^+$ and $[Pt(dppma)_2]^{2+}$ mole fractions of 0.343 and 0.657 (X = I) and 0.119 and 0.881 (X = Cl) respectively. Equilibrium constants of $K_{assoc} = 3.15 \times 10^{-1}$

* The assumptions are made that the measured $^1J(P–Pt)$ coupling constants are positive quantities which are invariant with the nature of the solvent and that the solution concentrations of $[Pt(dppma)_2X_2]$ are negligible.

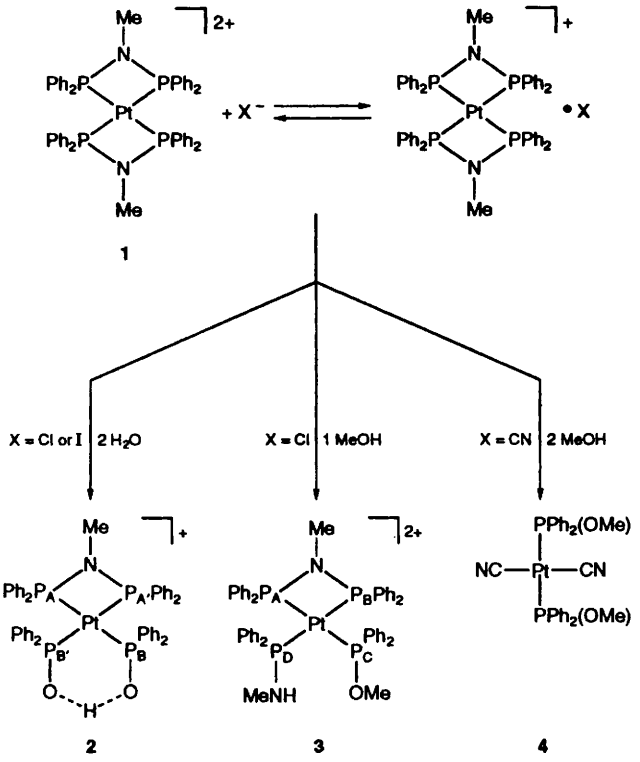

Scheme 1 Synthetic routes to products **2**–**4**; the phosphorus atoms of **2** and **3** are labelled with reference to the ^{31}P NMR spectroscopic assignments of Table 1

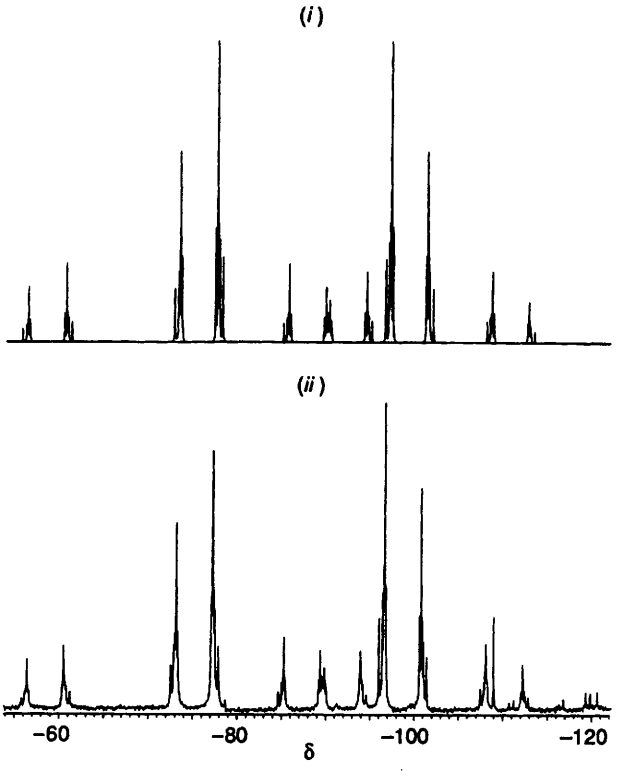

Fig. 1 Calculated (*i*) and observed (*ii*) ^{31}P-{^1H} NMR spectra of the hydrolysis product **2**

(X = I) and 7.18×10^{-2} mol dm^{-3} (X = Cl) in $MeNO_2$ are calculated from the mole fractions for equilibrium (2). The nature of the interaction of the chloride ion with **1** is evidently weaker than that of iodide as it effects a smaller increase in the magnitude of the Pt–P coupling of the free complex and also possesses a smaller equilibrium constant of association.

The association of halide to bis(chelate) dppm and dppa complexes yielding five-co-ordinate platinum(II) complexes is thought to arise from the specific steric conditions afforded by the two rigid four-membered rings[6] in which the phenyl substituents are unable to attain an axial displacement which may inhibit halide association. It is not observed[11] in the halide salts of $[Pt(dppe)_2]^{2+}$ (dppe = $Ph_2PCH_2CH_2PPh_2$) in which the additional methylene moiety of the ligand's backbone provides the five-membered ring with the necessary range of motion to obtain axial and equatorial displacement of its phosphorus substituents and therefore effectively prevent association of halide.

Synthesis and Solid-state Structure of [Pt(dppma)-{$(Ph_2PO)_2H$}]$I_{0.21}[BF_4]_{0.79}$.—The cationic complex [Pt-(dppma){$(Ph_2PO)_2H$}]$^+$ **2** was initially isolated as a halide salt by allowing a wet CH_2Cl_2 solution of either (X = Cl or I) halide salt of **1** to stand for several days (Scheme 1). The demonstrated facility of P–N bond solvolysis in both free[1] and co-ordinated[4] phosphazanes suggested adventitious water as the reagent in the cleavage of the P–N bonds of the complex. The absence of reaction of dry CH_2Cl_2 solutions of **1** upon standing for several days established the stability of the halide salts of **1** in dry aprotic solvents. The required presence of water to obtain the product was confirmed by its formation upon the addition of a trace amount of water to such a solution. The conspicuous piscine aroma of free amine which was liberated by the reaction supports the hydrolysis of the ligand's two P–N bonds to yield NH_2Me as a reaction by-product.

Spectral simulation[12] [Fig. 1(*i*)] effectively reproduced the complex ^{31}P-{^1H} NMR spectrum of the product [Fig. 1(*ii*)] as an AA'BB'/AA'BB'X spin system in which the two sets of chemically equivalent phosphorus nuclei are situated *cis* to one another. The preservation of one of the four-membered rings of **1** in the product is evident in the chemical shift of the upfield resonance which is similar to that of the tetrafluoroborate salt of **1** and its characteristically[6] small $|^1J(P–Pt)|$ coupling constant. The derived chemical shift and coupling-constant information is provided in Table 1.

The inertness of the tetrafluoroborate salt of complex **1** in wet CH_2Cl_2 * demonstrates that the presence of halide is necessary for P–N bond hydrolysis to proceed. Addition of 1 equivalent of NBu^n_4I to such a solution gave the reaction product as a mixture of the BF_4^- and I^- salts in a crystalline form suitable for an X-ray diffraction study. The geometry of **2** is illustrated in the ORTEP[13] representation (Fig. 2). Positional parameters for **2** and its counter ions are provided in Table 5, selected bond lengths and angles in Table 6. The crystal data and pertinent parameters are summarised in Table 7.

The crystals consist of discrete ions of [Pt(dppma)-{$(Ph_2PO)_2H$}]$^+$ and its counter ions. The shortest close contact between non-H atoms of the ion pair is 3.15(3) Å. The salt exhibited a crystallographic disorder involving partial site occupancies of 0.21 and 0.79 for the iodide and tetrafluoroborate anions, respectively. The geometry obtained for the BF_4^- anion suggested the presence of additional disorder associated with its orientation in the lattice; no attempts were made to model this disorder. The cation is best described as a square-planar complex which exhibits the expected distortion from an ideal geometry associated with the formation of one four-membered ring.[6] The planarity at the metal centre is effectively maintained with the platinum atom displaying the largest deviation [0.0544(8) Å] from the PtP_4 plane.

The four-membered ring of the dppma chelate exhibits similar structural features to those observed in the previously

* The complex exhibited no P–N bond hydrolysis upon standing in wet CH_2Cl_2 for 2 weeks.

Table 5 Positional parameters of complex **2**

Atom	*x*	*y*	*z*	Atom	*x*	*y*	*z*
Pt	0.190 31(4)	0.197 44(5)	0.484 22(5)	C(46)	0.195 5(11)	0.171 8(10)	0.699 1(11)
P(1)	0.278 3(3)	0.081 7(3)	0.500 6(3)	C(51)	0.107 1(11)	0.355 3(12)	0.577 3(11)
P(2)	0.296 5(3)	0.210 4(4)	0.598 9(3)	C(52)	0.165 6(13)	0.400 1(14)	0.628 2(13)
P(3)	0.117 3(3)	0.322 6(3)	0.483 0(3)	C(53)	0.160 0(14)	0.421 2(15)	0.703 8(13)
P(4)	0.104 7(3)	0.166 4(3)	0.363 2(3)	C(54)	0.090 4(13)	0.390 5(15)	0.726 1(14)
O(1)	0.026 9(8)	0.320 4(9)	0.432 9(8)	C(55)	0.030 5(15)	0.345(2)	0.677 6(15)
O(2)	0.015 5(7)	0.200 5(9)	0.347 9(7)	C(56)	0.036 9(14)	0.325 5(15)	0.604 1(14)
N	0.349 6(8)	0.130 0(9)	0.571 0(8)	C(61)	0.173 4(11)	0.407 8(13)	0.448 2(11)
C	0.429 4(12)	0.092 6(14)	0.614 1(13)	C(62)	0.249 5(13)	0.393 2(15)	0.430 6(13)
C(11)	0.248 8(12)	−0.013 0(12)	0.541 4(11)	C(63)	0.291 1(15)	0.461(2)	0.407 8(14)
C(12)	0.182 1(13)	−0.010 8(15)	0.576 4(13)	C(64)	0.259(2)	0.543(2)	0.411(2)
C(13)	0.160 4(15)	−0.082(2)	0.610 7(14)	C(65)	0.184(2)	0.555(2)	0.427 1(15)
C(14)	0.198 9(14)	−0.154(2)	0.607 6(14)	C(66)	0.138 3(14)	0.486 7(15)	0.448 2(14)
C(15)	0.267 0(15)	−0.158(2)	0.576 8(14)	C(71)	0.152 7(10)	0.204 4(13)	0.285 9(10)
C(16)	0.293 5(13)	−0.086 9(14)	0.543 8(12)	C(72)	0.237 3(12)	0.213 9(13)	0.297 0(12)
C(21)	0.331 1(11)	0.050 7(12)	0.426 4(11)	C(73)	0.271 8(13)	0.236 8(13)	0.236 3(12)
C(22)	0.395 5(11)	0.099 2(13)	0.411 9(11)	C(74)	0.216 5(13)	0.254 2(13)	0.164 6(13)
C(23)	0.429 4(13)	0.080 9(14)	0.349 0(12)	C(75)	0.133 3(13)	0.244 3(14)	0.152 2(14)
C(24)	0.395 5(13)	0.019 8(14)	0.299 0(14)	C(76)	0.100 3(12)	0.218 8(12)	0.213 1(11)
C(25)	0.332 1(12)	−0.030 1(13)	0.311 4(12)	C(81)	0.090 4(11)	0.056 5(12)	0.347 7(11)
C(26)	0.297 9(12)	−0.015 8(13)	0.376 0(12)	C(82)	0.057 4(13)	0.012 0(15)	0.400 2(13)
C(31)	0.363 9(10)	0.299 1(12)	0.616 6(10)	C(83)	0.039 5(14)	−0.072(2)	0.387 5(14)
C(32)	0.408 1(11)	0.317 3(14)	0.561 7(12)	C(84)	0.054 6(14)	−0.113(2)	0.325 3(14)
C(33)	0.452 8(14)	0.393 6(15)	0.564 1(14)	C(85)	0.089 0(12)	−0.072 0(14)	0.274 8(13)
C(34)	0.449 7(13)	0.450 5(15)	0.623 7(13)	C(86)	0.109 6(12)	0.014 5(13)	0.284 1(12)
C(35)	0.405 5(13)	0.430 2(15)	0.680 0(13)	H	0.054(8)	0.279(9)	0.367(8)
C(36)	0.365 4(11)	0.354 0(12)	0.677 0(11)	I	0.527 5(8)	0.292 4(9)	0.401 4(7)
C(41)	0.278 7(11)	0.182 3(12)	0.691 9(11)	F(1)	0.542 2(10)	0.228 7(11)	0.458 1(11)
C(42)	0.342 8(12)	0.165 8(12)	0.755 5(11)	F(2)	0.439 2(11)	0.308 3(14)	0.390 6(10)
C(43)	0.324 7(12)	0.138 3(12)	0.826 7(13)	F(3)	0.532 5(13)	0.255 0(13)	0.330 5(11)
C(44)	0.241 0(14)	0.128 1(14)	0.829 6(14)	F(4)	0.572(2)	0.353 6(14)	0.420(2)
C(45)	0.179 0(13)	0.142 8(13)	0.768 4(12)	B	0.526(12)	0.284(11)	0.398(10)

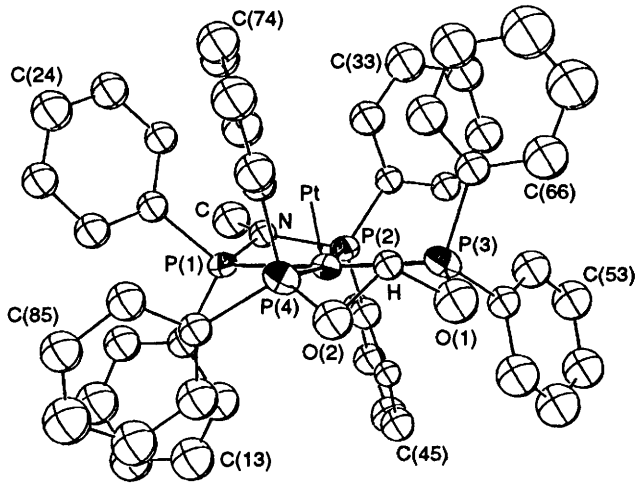

Fig. 2 An ORTEP representation of $[Pt(dppma)\{(Ph_2PO)_2H\}]^+$ **2** showing the atom numbering scheme. Thermal ellipsoids represent 50% probability contours. Anions have been omitted for clarity

described diphenylphosphinoamine chelate complexes of platinum(II).[6] Within the four-membered ring, the P–Pt–P bond angle of 69.4(2)° agrees favourably with that of 69.75(5)° observed in **1**. The P–N bond lengths of **2** are identical, within 2σ, to the P–N bond lengths of the starting material. The average of the indistinguishable Pt–P–N bond angles of 91.8(5) [P(1)] and 90.8(5)° [P(2)] is identical to that found in **1**. Ring strain in the four-membered ring is evident[6] in the 0.37(2) Å displacement of the methyl carbon atom from the NP_2 plane. The bond angles between the phenyl and amino substituents are consistent with a tetrahedral geometry at each phosphorus centre which involves the formation of a non-linear dative bond to the platinum atom of the strained ring.[6]

Table 6 Selected bond distances (Å) and angles (°) for complex **2**

Pt–P(1)	2.336(5)	P(3)–O(1)	1.547(15)
Pt–P(2)	2.359(5)	P(3)–C(51)	1.79(2)
Pt–P(3)	2.341(6)	P(3)–C(61)	1.84(2)
Pt–P(4)	2.324(6)	P(4)–O(2)	1.534(14)
P(1)–N	1.689(15)	P(4)–C(71)	1.83(2)
P(1)–C(11)	1.80(2)	P(4)–C(81)	1.79(2)
P(1)–C(21)	1.80(2)	O(1)–H	1.50(14)
P(2)–N	1.697(15)	O(2)–H	1.42(14)
P(2)–C(31)	1.79(2)	N–C	1.49(3)
P(2)–C(41)	1.79(2)		
P(1)–Pt–P(2)	69.4(2)	Pt–P(3)–O(1)	114.3(6)
P(1)–Pt–P(3)	171.4(2)	Pt–P(3)–C(51)	113.7(7)
P(1)–Pt–P(4)	99.8(2)	Pt–P(3)–C(61)	110.3(7)
P(2)–Pt–P(3)	102.1(2)	O(1)–P(3)–C(51)	104.6(9)
P(2)–Pt–P(4)	168.3(2)	O(1)–P(3)–C(61)	108.7(9)
P(3)–Pt–P(4)	88.5(2)	C(51)–P(3)–C(61)	104.7(9)
Pt–P(1)–N	91.8(5)	Pt–P(4)–O(2)	116.1(6)
Pt–P(1)–C(11)	120.4(7)	Pt–P(4)–C(71)	109.7(6)
Pt–P(1)–C(21)	121.4(7)	Pt–P(4)–C(81)	112.5(7)
N–P(1)–C(11)	107.5(8)	O(2)–P(4)–C(71)	108.2(8)
N–P(1)–C(21)	106.9(8)	O(2)–P(4)–C(81)	103.7(9)
C(11)–P(1)–C(21)	106.2(9)	C(71)–P(4)–C(81)	106.1(9)
Pt–P(2)–N	90.8(5)	P(3)–O(1)–H	92(6)
Pt–P(2)–C(31)	121.9(6)	P(4)–O(2)–H	85(6)
Pt–P(2)–C(41)	121.2(7)	P(1)–N–P(2)	104.2(8)
N–P(2)–C(31)	108.4(8)	P(1)–N–C	125.0(13)
N–P(2)–C(41)	106.1(8)	P(2)–N–C	128.0(13)
C(31)–P(2)–C(41)	105.6(9)	O(1)–H–O(2)	113(9)

Replacement of one of the dppma ligands of complex **1** with the diphenylphosphinous acid–diphenylphosphinite ligand of **2** results in elongation of the Pt–P bonds to the remaining dppma ligand. The average 2.348(4) Å separation of the platinum centre from the phosphorus atoms of the dppma ligand is > 10σ greater than the longest Pt–P bond of the previously

Table 7 X-Ray experimental details for complexes **2** and **4**

	2	**4**
Empirical formula	$C_{49}H_{44}B_{0.79}F_{3.16}I_{0.21}NO_2P_4Pt$	$C_{28}H_{26}N_2O_2P_2Pt$
M	1093.14	679.59
a/Å	16.491(6)	7.327(2)
b/Å	16.070(4)	16.730(4)
c/Å	17.642(5)	10.728(2)
β/°	103.38(3)	95.71(2)
U/Å^3	4548(5)	1308(1)
Z	4	2
Crystal dimensions (mm)	0.12 × 0.18 × 0.12	0.14 × 0.10 × 0.16
Space group (crystal system)	$P2_1/n$ (monoclinic)	$P2_1/c$ (monoclinic)
D_c/g cm^{-3}	1.60	1.72
μ/cm^{-1}	37.6	55.6
2θ range (°)	2–44	2–56
Unique reflections: measured	5994	3371
$I > 3\sigma(I)$	2742	1860
Number of parameters	307	103
R	0.053	0.035
R'	0.054	0.044
E.s.d. of observation of unit weight	1.15	1.13

characterised bis(diphenylphosphino)amine chelate complexes of Pt^{II}.[6] The average 2.333(4) Å length of the Pt–P bonds to the $Ph_2POHOPPh_2$ ligand of **2** also is longer than those observed[14,15] in other crystallographically characterised platinum(II) complexes of this ligand. An asymmetry in the lengths of the Pt–P bonds is observed with both ligands; the longer metal bond of each ligand is situated *trans* to the shorter Pt–P bond of the other ligand. No chemical significance is associated with the disparity.

The six-membered ring of the diphenylphosphinous acid–diphenylphosphinite ligand obtains a near-ideal P–Pt–P bond angle of 88.5(2)°. The five non-hydrogen atoms of the ring are not planar. The P(3)–Pt–P(4)–O(2) dihedral angle of 31.4(6)° is the largest within the ring. The eclipsed orientation of the oxygen atoms and their 2.42(2) Å separation suggests the presence of strong hydrogen bonding between them and a bridging hydrogen atom. The solid-state structures of [Pt(Ph$_2$PCH$_2$CH$_2$)(Ph$_2$POHOPPh$_2$)] and [Pt$_2$(μ-H)(μ-PPh$_2$)(Ph$_2$POHOPPh$_2$)$_2$] exhibit respective O···O distances of 2.476(8)[15] and 2.424(10) and 2.429(10) Å.[15] Refinement of the site of the bridging hydrogen atom produced a symmetric displacement between the oxygen atoms [O(1)–H 1.50(14), O(2)–H 1.42(14) Å]. Its location however is not considered to be reliable because of its large disposition, in the absence of other hydrogen-bonding contacts, from the O···O vector [O–H–O 113(9)°].

Allowing a wet CH_2Cl_2 solution of the chloride salt of complex **1** to stand for several months results in further ligand hydrolysis. The complex [Pt(Ph$_2$POH)(Ph$_2$POHOPPh$_2$)Cl] has been identified as a reaction product.[16]

Spectroscopic Identification of the Complex [Pt(dppma)(Ph$_2$POMe)(Ph$_2$PNHMe)]$^{2+}$ **3**.—The formation of the intermediate anticipated in cleavage of one of the P–N bonds of complex **1** *en route* to the synthesis of **2** is not evident in the monitoring *via* ^{31}P NMR spectroscopy of the reaction of the chloride and iodide salts of **1** with water. The use of methanol as the protic solvent in the reaction with the chloride and tetrafluoroborate salts permitted the isolation of the product of single P–N bond solvolysis and demonstrated the general nature of P–N bond reactivity in **1**. The yellow CH_2Cl_2 solution of the chloride salt of **1** discolours upon standing ($t_{\frac{1}{2}} \approx 3$ h) after the addition of several drops of MeOH. Methanolysis of the chloride salt occurs at a rate which is at least an order of magnitude faster than the rate of methanolysis of free dppma ($t_{\frac{1}{2}} \approx 50$ h). The ^{31}P-{^{1}H} NMR spectrum of the reaction solution after 12 h, shown in Fig. 3(*ii*), consists almost

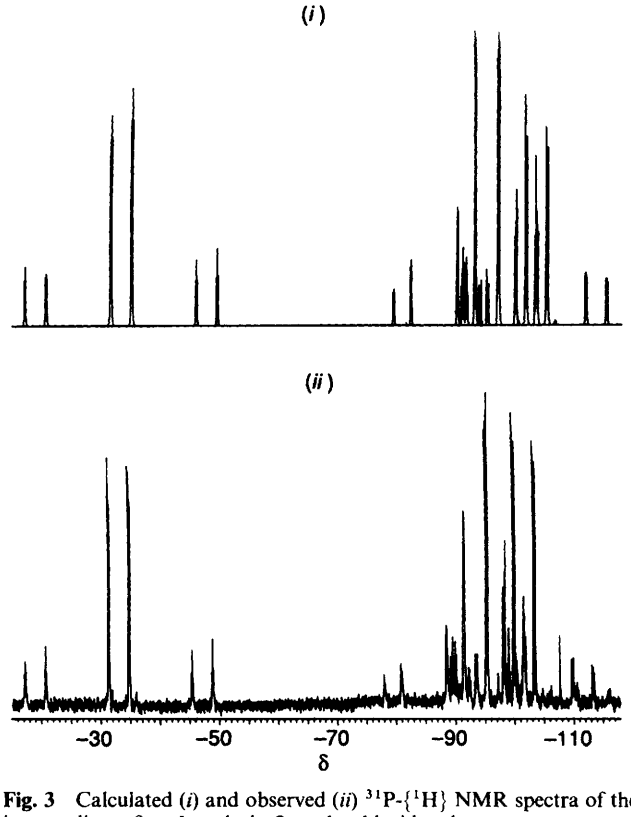

Fig. 3 Calculated (*i*) and observed (*ii*) ^{31}P-{^{1}H} NMR spectra of the intermediate of methanolysis, **3**, as the chloride salt

exclusively of the product [Pt(dppma)(Ph$_2$POMe)(Ph$_2$PNHMe)]$^{2+}$ **3** (see Scheme 1). Further solvolysis of the starting material to yield the methoxy analogue of **2**, [Pt(dppma)(Ph$_2$POMe)$_2$]$^{2+}$, is not observed.

The ^{31}P NMR spectrum represents an ABCD/ABCDX spin system in which each of the phosphorus resonances consists of a doublet of doublets of doublets with ^{195}Pt-coupled satellites. Spectral simulation[12] gave the spectrum in Fig. 3(*i*). The derived chemical shift and coupling constant data are given in Table 1. The two chemically inequivalent resonances of the dppma ligand possess the smallest $|^1J$(P–Pt)| coupling constants and the greatest upfield chemical shifts of the complex.[6]

Examination of its FAB mass spectrum exclusively did not

permit the verification of complex **3** as the product of solvolysis of one P–N bond of **1**. However, the increase in mass of the molecular ion of the deuteriated analogue $[Pt(dppma)(Ph_2POCD_3)(Ph_2PNDMe)]^{2+}$ prepared from the reaction of the chloride salt of **1** with CD_3OD is consistent with the incorporation of four deuterium atoms into the complex and, in conjunction with the fragmentation pathway of the deuteriated complex, confirms the addition of methanol across the P–N bond.

Synthesis and Solid-state Structure of trans-$[Pt(Ph_2POMe)_2(CN)_2]$ **4**.—The complex *trans*-$[Pt(Ph_2POMe)_2(CN)_2]$ **4**, rather than the anticipated[6] product *trans*-$[Pt\{Ph_2PN(Me)PPh_2\}_2(CN)_2]$, was synthesised in high yield from the treatment of a CH_2Cl_2 solution of **1** with 2 equivalents of methanolic sodium cyanide. The $^{31}P-\{^1H\}$ NMR chemical shift and $^1J(Pt–P)$ coupling constant data are reported in Table 1. The concurrent formation of Ph_2POMe, observed in the ^{31}P NMR spectrum as a reaction by-product, with **4** represents the complete methanolysis of the dppma ligands of **1**. The identity of **4** as the reaction product was spectroscopically confirmed by its independent synthesis from the reaction of *trans*-$[Pt(PPh_2OMe)_2Cl_2]$ with NaCN.

Crystals suitable for a crystallographic determination of complex **4** were subsequently obtained from the former reaction. An ORTEP representation of **4** is given in Fig. 4. Positional parameters and selected bond distances and angles are provided in Tables 8 and 9, respectively. The crystal data and details of the structure determination are given in Table 7. The crystal structure consists of discrete molecules of *trans*-$[Pt(Ph_2POMe)_2(CN)_2]$ which possess a crystallographically imposed centre of inversion. The P–Pt–C bond angle of 90.3(2)° infers an almost ideal square-planar geometry at the metal centre.

As seen in Fig. 4, the conformation adopted by the ligands about the metal centre results in the displacement of one of the phenyl substituents of each phosphine to a position which is effectively perpendicular to the PtP_2C_2 co-ordination plane. This is in contrast to the arrangement about the platinum centre of *trans*-$[Pt(dppa)_2(CN)_2]$[6] in which the PtP_2C_2 co-ordination plane approximately bisects the angle between the phenyl substituents of the monodentate phosphine ligands.

The bond lengths and angles within the methoxydiphenyl phosphine ligands of complex **4** are very similar to those observed in the ligands of the square-pyramidal complex *cis*-$[Rh(NO)(Ph_2POMe)_2Br_2]$.[17] The structures of the cyano and phenyl groups of **4** are normal.[18]

The manner by which complexes **2**–**4** are obtained is not known. However, the required participation of halide ions to obtain **2** and **3** and the presence of the cyano ligands in **4** suggests a common initial reaction pathway in which formation of a five-co-ordinate species, as observed in the association of **1** with halide and cyanide[6] respectively, classically represents the first step of associative substitution in square-planar platinum(II) complexes.[19] Although it could not be identified spectroscopically,[6] the complex of cyanide substitution, *trans*-$[Pt(dppma)_2(CN)_2]$, is thought to be the reaction intermediate which undergoes P–N bond cleavage on the pathway to formation of **4** as it is consistent with the observed formation of *trans*-$[Pt(dppa)_2(CN)_2]$ from $[Pt(dppa)_2]^{2+}$ and NaCN under the same reaction conditions. Similarly, the presence of chloride as a ligand of platinum in the hydrolysis product of **1**, $[Pt(Ph_2POH)(Ph_2POHOPPh_2)Cl]$,[16] shows that halide substitution also occurs in these complexes.

Cyanide or halide substitution in complex **1** to yield monodentate dppma may then be followed by P–N bond cleavage of the ligand by the protic solvent; P–N bond solvolysis of both the co-ordinated and unco-ordinated phosphine moieties of monodentate diphosphinoamines has previously been demonstrated.[5] The presence of only trace quantities of species other than the products **2**–**4** in the ^{31}P NMR spectrum of their reaction solutions at intermediate times precludes an unambiguous characterisation of the remaining steps of P–N bond cleavage.

In obtaining products **3** and **2**, however, the cleavage of one and both P–N bonds of a dppma ligand of $[Pt(dppma)_2]X_2$ upon reaction with MeOH and water respectively suggests that the inability to observe spectroscopically the product of single P–N bond hydrolysis as an intermediate to the formation of **2** may arise from an intrinsic difference in its structure from that

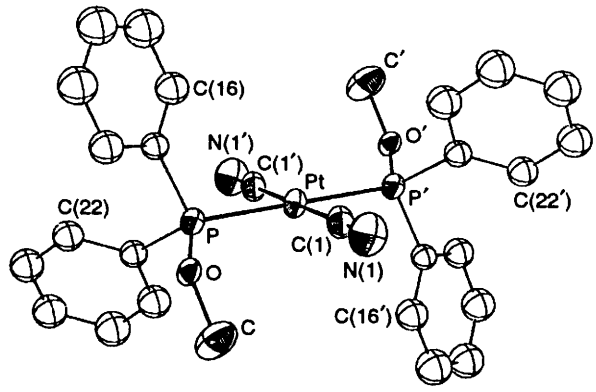

Fig. 4 An ORTEP diagram of *trans*-$[Pt(Ph_2POMe)_2(CN)_2]$ **4** showing the atom numbering scheme. Thermal ellipsoids represent 50% probability contours

Table 8 Positional parameters of complex **4**

Atom	*x*	*y*	*z*
Pt	0	0	0
P	0.027 3(3)	0.014 50(9)	0.214 3(2)
O	−0.160 3(8)	0.029 3(4)	0.275 2(5)
N(1)	0.363(1)	−0.101 8(5)	0.017 2(8)
C	−0.309(1)	−0.027 2(7)	0.256(1)
C(1)	0.230(1)	−0.064 9(5)	0.011 7(7)
C(11)	0.156(1)	0.102 7(4)	0.263 7(7)
C(12)	0.119(1)	0.143 1(5)	0.372 4(8)
C(13)	0.215(1)	0.212 2(6)	0.406(1)
C(14)	0.347(2)	0.239 8(6)	0.336(1)
C(15)	0.385(2)	0.199 5(6)	0.232(1)
C(16)	0.291(1)	0.129 2(5)	0.194 0(8)
C(21)	0.135(1)	−0.067 2(4)	0.302 6(7)
C(22)	0.252(1)	−0.056 1(5)	0.411 2(8)
C(23)	0.320(1)	−0.121 1(5)	0.480 6(9)
C(24)	0.268(1)	−0.196 6(5)	0.445 0(9)
C(25)	0.153(1)	−0.209 5(6)	0.337(1)
C(26)	0.089(1)	−0.146 2(5)	0.266 0(9)

Table 9 Selected bond distances (Å) and angles (°) for complex **4**

Pt–P	2.301(2)	P–C(21)	1.801(7)
Pt–C(1)	1.995(8)	O–C	1.442(11)
P–O	1.599(6)	N(1)–C(1)	1.153(10)
P–C(11)	1.801(7)		
P–Pt–C(1)	90.3(2)	C(12)–C(13)–C(14)	120.7(9)
Pt–P–O	115.6(2)	C(13)–C(14)–C(15)	120(1)
Pt–P–C(11)	111.8(2)	C(14)–C(15)–C(16)	121(1)
Pt–P–C(21)	115.8(3)	C(11)–C(16)–C(15)	118.2(8)
O–P–C(11)	101.5(3)	P–C(21)–C(22)	122.8(6)
O–P–C(21)	104.7(3)	P–C(21)–C(26)	118.9(6)
C(11)–P–C(21)	106.1(4)	C(22)–C(21)–C(26)	118.1(7)
P–O–C	120.6(6)	C(21)–C(22)–C(23)	120.4(7)
Pt–C(1)–N(1)	179.1(7)	C(22)–C(23)–C(24)	120.2(9)
P–C(11)–C(12)	120.2(6)	C(23)–C(24)–C(25)	120.6(9)
P–C(11)–C(16)	119.3(6)	C(24)–C(25)–C(26)	119.8(9)
C(12)–C(11)–C(16)	120.5(7)	C(21)–C(26)–C(25)	120.9(9)
C(11)–C(12)–C(13)	119.2(8)		

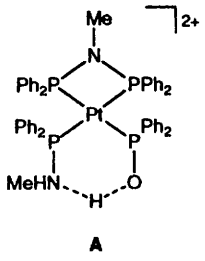

A

of **3** which results in its greater reactivity to further P–N bond hydrolysis. Intramolecular proton transfer in the formation of a six-membered ring **A** analogous to that observed in the final product is thought to facilitate cleavage of the intermediate's P–N bond as it provides a high effective concentration of acidic H^+. As no such corresponding pathway exists for cleavage of the P–N bond of **3**, the complex possesses a kinetic stability which permits its isolation.

Conclusion

Conductivity measurements and ^{31}P NMR spectroscopic studies have shown that the halide salts of the bis(chelate) complex **1** form the five co-ordinate species $[Pt(dppma)_2X]^+$ (X = Cl or I) in solution which exist in equilibrium with the unassociated form of **1**. The position of this equilibrium is dependent upon the nature of the solvent in which the salts are dissolved. The interaction of iodide with **1** is apparently greater than that of the chloride counter-ion as both its equilibrium constant of association and its perturbation of the ^1J(P–Pt) coupling in $[Pt(dppma)_2]^{2+}$ are larger than that observed for the chloro complex.

Characterisation of the complexes **2**–**4** demonstrates a susceptibility of the P–N bonds of the dppma ligands of **1** to solvolysis. The P–N bond-cleavage reactions exhibit a dependence upon the presence of nucleophiles supplemental to the protic reagents. Although the intimate mechanisms by which solvolysis proceeds to obtain these complexes are not yet fully understood, substitution of these nucleophiles in **1** is thought to be a common first step to formation of the final products.

Experimental

All reactions were performed in air, except where stated. Reactions which proved to be water-sensitive were carried out in an inert atmosphere of N_2 using solvents which were dried using standard techniques.[20]

The ^{31}P NMR spectra were recorded on a Varian XL-200 spectrometer operating at 81.0 MHz or a Varian Gemini 300 spectrometer operating at 121.5 MHz. The ^{31}P-{^1H} NMR chemical shifts were measured with reference to external $P(OMe)_3$ in C_6D_6 or $(CD_3)_2CO$ and are reported with reference to 85% H_3PO_4. Fast-atom bombardment (FAB) mass spectrometric analyses were performed in a nitrobenzyl alcohol matrix using a Varian VG70-250S mass spectrometer with a Xe gas ionising source, 8 kV and 1 mA.

Solvents and common reagents were obtained from the Aldrich, BDH or Fischer chemical companies. The $K_2[PtCl_4]$ starting material was obtained from Strem Chemicals Inc. $[Pt(cod)Cl_2]$, $[Pt(cod)I_2]$ and $[Pt(cod)_2]$ (cod = cycloacta-1,5-diene) were synthesised using the techniques of Whitesides and co-workers,[21] Drew and Doyle,[22] and Spencer[23] respectively. The bis(diphenylphosphino)amine and bis(diphenylphosphino)methylamine ligands were prepared following the method of Wang *et al.*[24] The synthesis of **1** has been described previously.[6]

[*Bis(diphenylphosphino)methylamine*] [*hydrogenbis(diphenylphosphinite)*] *platinum*(II) *Iodide Tetrafluoroborate* (1/0.21/0.79) **2**.—The addition of NBu^n_4I (74 mg, 0.20 mmol) as a solid to a colourless suspension of $[Pt(dppma)_2][BF_4]_2$ (233 mg, 0.200 mmol) in CH_2Cl_2 (20 cm^3) gave a clear yellow-orange solution. After adding a drop of distilled water, the solution was allowed to stand for 10 d during which the original intense colour faded to pale yellow. Reaction was also evident in the piscine aroma of free amine. The solution was then concentrated under reduced pressure to a volume of approximately 5 cm^3. The product was precipitated as a pale yellow solid by dropwise addition of cold Et_2O (20 cm^3). The product, collected by filtration and washed with cold Et_2O (5 cm^3), was obtained in 65% yield.

[*Bis(diphenylphosphino)methylamine*][*(diphenylphosphino)-methylamine*](*methoxydiphenylphosphine*)*platinum*(II) *Dichloride* **3**.—Several drops of MeOH were added to a solution of $[Pt(dppma)_2]Cl_2$ (213 mg, 0.200 mmol) in CH_2Cl_2 (20 cm^3) while ensuring that the resultant solution retained a yellow hue. On allowing the solution to stand for 24 h it turned colourless. Reduction in the solvent volume to approximately 10 cm^3 followed by slow addition of Et_2O (20 cm^3) induced precipitation of the product as a white solid. This was filtered off and washed with Et_2O (5 cm^3). Yield: 70%.

trans-Dicyanobis(methoxydiphenylphosphine)platinum(II) **4**.—*Method* 1. The reaction solution obtained by the addition of NaCN (12 mg, 0.250 mmol) in MeOH (10 cm^3) to a CH_2Cl_2 solution (25 cm^3) of $[Pt(dppma)_2][BF_4]_2$ (146 mg, 0.125 mmol) was allowed to stand for 36 h. The initial faint yellow colour observed upon addition of the reagents disappeared during the course of reaction. Reduction in solvent volume under reduced pressure caused precipitation of the product. Isolation by filtration followed by washing of the product with MeOH (5 cm^3) and tetrahydrofuran (5 cm^3) gave **4** as a white solid in 80% yield.

Method 2. A solution of $PPh_2(OMe)$ (216 mg, 1.00 mmol) in CH_2Cl_2 (5 cm^3) was added to a CH_2Cl_2 solution (25 cm^3) of $[Pt(cod)Cl_2]$ (187 mg, 0.500 mmol). The resulting colourless solution was stirred for 15 min. The addition of a methanolic solution (25 cm^3) of NaCN (49 mg, 1.00 mmol) in a dropwise manner over a period of 10 min induced the precipitation of the NaCl by-product. After stirring for 15 min, the solvent was removed to dryness. The product was redissolved in the minimum volume of CH_2Cl_2 and filtered. The solid collected by removal of the filtrate solvent to dryness was recrystallised from MeOH to give the colourless product in 84% yield.

Conductivity Measurements.—Conductivity measurements were made using a SYBRON/Barnstead PM-70CB conductivity bridge. Using the cell constant provided with the Copenhagen Radiometer CDC 104–41 conductivity cell, the molar conductivities of the platinum salt solutions were obtained at 25 °C in the concentration range 10^{-4}–10^{-2} mol dm^{-3}. In preparing the solutions, samples of the freshly prepared chloride, iodide and tetrafluoroborate salts of complex **1** were weighed out analytically on a Mettler B5 analytical balance. The solutions were obtained by dilution of the most concentrated stock solution. The nitromethane solvent was purified by collection of the middle fraction of its distillate in air. The measured background conductivity of 0.60 mS cm^{-1} so obtained is well within accepted standards.[7] The measured conductance, presented as a function of concentration, for the tetrafluoroborate, chloride and iodide salts of **1** is reported in Table 2.

X-Ray Data Collection and Structure Solution.—The unit-cell dimensions and the integrated intensities of reflections of the crystal structures were measured at 295 K using an Enraf-Nonius CAD-4F diffractometer with graphite-monochromated Mo-Kα radiation (λ = 0.710 73 Å). Calculations were carried out on a PDP 11/23 computer using SDP[25] and an Apollo

DSP 10020 minisupercomputer using the SHELX 76[26] and 86[27] packages. Neutral atom scattering factors were used as provided in the SDP[25] and SHELX 76[26] programs.

Complex **2**. Crystals of the complex were grown from CH_2Cl_2 solution by slow evaporation. A block-shaped crystal was mounted on a glass fibre. Accurate cell dimensions and the crystal orientation matrix were determined by a least-squares treatment of the setting angles of 21 reflections in the range $5 < \theta < 12°$. Intensities of reflections with indices h − 18 to 18, k 0–17, l 0–19 were measured using ω–2θ scans with a scan width of $(0.80 + 0.35 \tan \theta)°$ in ω; no decay correction was applied as the intensities of three standard reflections measured approximately every 4 h of X-ray exposure showed a decrease in intensity of less than 2% during data collection. The space group was determined by the systematic absences ($0k0$ absent if $k = 2n + 1$, $h0l$ absent if $h + l = 2n + 1$). The 5994 measured reflections were corrected for Lorentz and polarisation effects. An absorption correction was applied to the data using the program DIFABS.[28] 2742 Data with $I > 3\sigma(I)$ were labelled observed and used in the structure solution and refinement.

The structure was solved by the heavy-atom method. Refinement was by full-matrix least-squares calculations, initially with isotropic and then with anisotropic thermal parameters for the Pt, P, F and I atoms. Crystallographic disorder was exhibited in the partial occupancies of the counter ion site by the BF_4^- and I^- anions. Modelling of the disorder proceeded *via* the initial determination of the position of the iodide ion. The resulting contribution to the phasing from that region of the unit cell permitted resolution of the fluorine and boron atoms. The site occupancy factor (s.o.f.) of the iodine atom, coupled to that of the boron atom, was refined independently of the s.o.f. of the fluorine atoms, yielding values of 0.21 and 0.78, respectively. Confidence in the value of the s.o.f. of the iodide ion was considered to be higher than in that of the fluorine atoms. The fluorine atom s.o.f. was therefore taken as $1 - 0.21 = 0.79$. The s.o.f.s were then fixed at these values and the positions of the atoms refined in the normal manner. The hydrogen atom bridging oxygens O(1) and O(2) was located from inspection of the Fourier-difference electron-density map and its position refined in the least-squares calculations. The remaining hydrogen atoms were positioned on geometric grounds and included (as riding atoms) in the structure-factor calculation. The final cycle of refinement converged with unweighted and weighted agreement factors to values of $R = 0.053$ and $R' = [\Sigma w(|F_o| - |F_c|)^2/\Sigma w F_o^2]^{\frac{1}{2}} = 0.054$ respectively where $w = 4F_o^2/\sigma^2(F_o^2)$. The maximum shift/e.s.d. in the final cycle of refinement was < 0.01; the highest peak in the final Fourier-difference map, 0.26 e Å^{-3}, was associated with O(1). No correction for secondary extinction was applied.

Complex **4**. Colourless crystals were grown from CH_2Cl_2–MeOH solution by slow evaporation. X-Ray data collection and structure refinement proceeded as above with the following exceptions. The cell dimensions and the crystal orientation matrix were obtained from the setting angles of 23 reflections in the range $11 < \theta < 15°$. Intensities of reflections with indices h 0–10, k 0–23, l −15 to 15 were measured using ω–2θ scans with a scan width of $(0.75 + 0.35 \tan \theta)°$ in ω. Two intensity standards measured approximately every 4 h of X-ray exposure showed a decrease in intensity of less than 1% during data collection. An empirical absorption correction was applied based upon ψ scans of six reflections with θ values in the range 4–22°. The transmission factors ranged from 68.37 to 99.88%. Equivalent reflections were averaged with $R = 0.017$.

Refinement proceeded initially with isotropic and then with anisotropic thermal parameters for Pt, P and the N and C atoms of the cyanide and methoxide groups. The final cycle of refinement converged with unweighted and weighted agreement factors to values of $R = 0.035$ and $R' = 0.044$ respectively where the non-Poisson weighting function, w, defined as $4F_o^2/[\sigma(F_o)^2 + (0.05F_o^2)^2]$ was used to downweight intense reflections. The maximum parameter shift/e.s.d. in the final cycle of refinement was $< 0.01 : 1$, the highest peak in the final Fourier-difference map (1.02 e Å^{-3}) at position (0.125, 0.000, −0.029) was associated with the Pt atom.

Additional material available from the Cambridge Crystallographic Data Centre comprises H-atom coordinates, thermal parameters and remaining bond lengths and angles.

Acknowledgements

We thank Dr. Alex Young for obtaining the mass spectra. Funding provided by the Natural Sciences and Engineering Research Council is also gratefully acknowledged.

References

1 E. S. Batyeva, V. A. Al'fonsov and A. N. Pudovik, *Chemistry of Organophosphorus Compounds*, ed. A. N. Pudovik, Mir Publishers, Moscow, 1989.
2 É. E. Nifant'ev and E. V. Borisov, *Zh. Obshch. Khim.*, 1985, **55**, 1660; *J. Gen. Chem. USSR (Engl. Transl.)*, 1985, **55**, 1478 and refs. therein.
3 A. A. Korkin and E. N. Tsvetkov, *Zh. Obshch. Khim.*, 1987, **57**, 2155; *J. Gen. Chem. USSR (Engl. Transl.)*, 1987, **57**, 1929.
4 R. B. King, *Acc. Chem. Res.*, 1980, **13**, 243 and refs. therein.
5 R. B. King and J. Gimeno, *Inorg. Chem.*, 1978, **17**, 2396.
6 C. S. Browning and D. H. Farrar, *J. Chem. Soc., Dalton Trans.*, 1995, 521.
7 W. J. Geary, *Coord. Chem. Rev.*, 1971, **7**, 81.
8 M. C. Grossel, R. P. Moulding, K. R. Seddon and F. J. Walker, *J. Chem. Soc., Dalton Trans.*, 1987, 705.
9 A. D. Westland and J. Plušćec, *Can. J. Chem.*, 1968, **46**, 2097.
10 A. G. Sharpe, *J. Chem. Educ.*, 1990, **67**, 309.
11 G. K. Anderson, J. A. Davies and D. J. Schoeck, *Inorg. Chim. Acta*, 1983, **76**, L251.
12 Locally modified version of QCPE Program No. 458, LAOCN-5: Analysis of Isotropic NMR Spectra of Spin-$\frac{1}{2}$ Systems, L. Cassidei and O. Sciacovelli, Department of Chemistry, University of Bari, Bari, 1984.
13 C. K. Johnson, ORTEP II Report ORNL 5138, Oak Ridge National Laboratory, Oak Ridge, TN, 1976.
14 Q.-B. Bao, S. J. Geib, A. L. Rheingold and T. B. Brill, *Inorg. Chem.*, 1987, **26**, 3453.
15 P. W. N. M. van Leeuwen, C. F. Roobeek, J. H. G. Frijns and A. G. Orpen, *Organometallics*, 1990, **9**, 1211.
16 R. A. Burrow, Ph.D. Dissertation, University of Toronto, 1995.
17 R. B. English, M. M. De V. Steyn and R. J. Haines, *Polyhedron*, 1987, **6**, 1503.
18 F. H. Allen, O. Kennard, D. G. Watson, L. Brammer, A. G. Orpen and R. Taylor, *J. Chem. Soc., Perkin Trans. 2*, 1987, S1.
19 M. L. Tobe, *Inorganic Reaction Mechanisms*, Thomas Nelson and Sons, London, 1972.
20 D. F. Shriver and M. A. Drezdzon, *The Manipulation of Air-sensitive Compounds*, 2nd edn., Wiley, Toronto, 1986.
21 J. X. McDermott, J. F. White and G. M. Whitesides, *J. Am. Chem. Soc.*, 1976, **98**, 6521.
22 D. Drew and J. R. Doyle, *Inorg. Synth.*, 1972, **13**, 50.
23 J. L. Spencer, *Inorg. Synth.*, 1979, **19**, 213.
24 F. T. Wang, J. Najdzionek, K. L. Leneker, H. Wasserman and D. M. Braitsch, *Synth. React. Inorg. Metal-Org. Chem.*, 1978, **8**, 119.
25 B. A. Frenz, SDP Structure Determination Package, College Station, TX and Enraf-Nonius, Delft, 1982.
26 G. M. Sheldrick, SHELX 76, Program for crystal structure determination and refinement, University of Cambridge, 1976.
27 G. M. Sheldrick, SHELX 86, Program for crystal structure determination, University of Göttingen, 1986.
28 N. Walker and D. Stuart, *Acta Crystallogr., Sect. A*, 1983, **39**, 158.

Received 14*th November* 1994; *Paper* 4/06902A